

Mass-transfer-limited nitrogen and phosphorus uptake by stream periphyton: A conceptual model and experimental evidence

Scott T. Larned,¹ Vladimir I. Nikora, and Barry J. F. Biggs

National Institute of Water and Atmospheric Research, P.O. Box 8602, Christchurch, New Zealand

Abstract

We conducted flow-tank experiments to examine nitrate (NO₃) and dissolved reactive phosphorus (DRP) uptake by stream periphyton over a wide range of near-bed velocities and turbulence levels. Our aims were to characterize the hydraulic conditions under which nutrient uptake is controlled by mass transfer through diffusive boundary layers (DBLs) or by membrane kinetics and to identify factors that affect mass-transfer rates. Nutrient uptake was mass-transfer limited under all hydraulic conditions used; there was no indication of kinetic control. We developed a conceptual model describing mass-transfer-limited uptake in terms of periphyton canopy height relative to DBL thickness. Three uptake regimes comprise the model: (1) when the canopy is submerged within the DBL covering the substratum, uptake is controlled by the thickness of this DBL; (2) when canopy height is greater than but comparable with the substratum DBL thickness, uptake is controlled jointly by the substratum DBL and by individual DBLs surrounding the periphyton elements that protrude above the substratum DBL; and (3) when the substratum DBL is very thin and most of the canopy protrudes above it, uptake is controlled by the DBLs surrounding periphyton elements. Patterns of NO₃ and DRP uptake in the experiments were consistent with the third regime. Periphyton extended well above the substratum DBL even at the slowest near-bed velocities (~1 cm s⁻¹). We suggest that, in oligotrophic streams, the second and third uptake regimes prevail, DBLs around periphyton elements pose greater diffusive resistance to nutrient transport than the substratum DBL, and nutrient uptake is generally mass-transfer controlled and rarely kinetically controlled.

Nutrient uptake by periphyton and other benthic autotrophs is controlled by three processes that occur in series: (1) rapid transport by turbulent diffusion from the mainstream into the viscous sublayer of the benthic boundary layer; (2) slower transport, dominated by molecular diffusion, through the inner portion of the viscous sublayer (the diffusive boundary layer, or DBL) to periphyton cell surfaces; and (3) membrane transport from cell surfaces into cells. The slowest of these processes poses the greatest resistance to nutrient transport and will control the rate of uptake (Nobel 1999). Transport toward the benthos by turbulent diffusion is very rapid in all but the slowest streams and will rarely be the rate-limiting step; either mass transfer through the DBL or membrane transport will limit uptake under most conditions (Sanford and Crawford 2000).

The viscous sublayer and the DBL embedded in it decrease in thickness with increasing mainstream velocity (Levich 1962). Consequently, mass-transfer control is expected at low velocities, and membrane-transport or kinetic control at higher velocities, when the DBL becomes so thin

that diffusion through it is faster than membrane transport (Jumars et al. 2001).

The critical DBL thickness at which uptake shifts between mass transfer and kinetic control corresponds to a saturating mainstream velocity (Wheeler 1980). Saturating velocities reported for inorganic carbon, nitrogen, and phosphorus uptake by marine and freshwater macroalgae range from 2 to 22 cm s⁻¹ (Wheeler 1980; Gerard 1982; Koch 1993; Borchardt et al. 1994; Hurd et al. 1996). Saturating velocities for uptake have not been determined for the thin mats and short filamentous canopies characteristic of unpolluted stream periphyton. Although periphyton communities are ubiquitous features in streams, studies of boundary-layer effects on nutrient uptake by stream periphyton are lacking. Boundary-layer effects on mass transfer in lentic algae have been examined, but those studies have employed laminar flow (e.g., Ribber and Wetzel 1987), an atypical condition in most streams.

In the present study, we developed a conceptual model and conducted experiments to examine interactions between periphyton stature, near-bed (top of periphyton canopy) flow conditions, and nutrient uptake. The model relates changes in periphyton stature and DBL thickness to nutrient uptake, as periphyton shift from complete submergence within the substratum DBL to protrusion into flow regions where turbulent diffusion enhances nutrient supply. We measured nitrate (NO₃) and dissolved reactive phosphorus (DRP) uptake in flow-tank experiments over a wide range of near-bed flows and determined the relationships between flow conditions and periphyton stature. Results of the experiments were evaluated in the context of the model.

Conceptual framework

Periphyton assemblages can have complex architectures and often grow on rough and/or porous substrata. A rigorous

¹ Corresponding author (s.larned@niwa.co.nz).

Acknowledgments

We thank David Gunn for assistance with ADV measurements and data analysis, Cathy Kilroy for identification and quantification of periphyton species, Alan Stokes for equipment fabrication, and the NIWA Christchurch laboratory staff for biomass analyses. We thank Robert Spiegel, Janelle Fleming, Jason Fleming, Josef Ackerman, and three anonymous reviewers for constructive manuscript reviews.

The study was conducted under contracts C01X0215 and C01X0308 from the Foundation for Research Science and Technology (New Zealand).

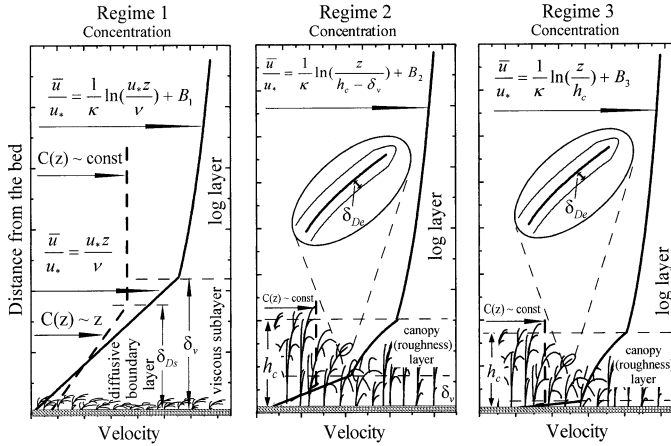


Fig. 1. Schematic diagrams showing mass-transfer-uptake regimes. Heavy dashed lines show linear distributions of concentration within the diffusive boundary layer (DBL) and constant concentrations above the DBL. Solid lines show velocity profiles in the viscous, roughness, and logarithmic layers. Governing relationships for portions of each profile are indicated by arrows. Equations are for vertical distributions of mean velocities and indicate hydraulically smooth flow in Regime 1 and slightly rough and fully rough flows in Regimes 2 and 3. Insets show a single periphyton element surrounded by a DBL.

theoretical approach for understanding mass-transfer processes under these conditions is not yet available. Therefore, we developed a model for simpler architectures dominated by filaments and diatom chains and clusters (for brevity, we refer to these structures as elements). This architecture was appropriate for the periphyton in our experiments and allowed us to parameterize the model using simple geometric shapes.

The model was developed for periphyton canopies on flat, impermeable beds in fully developed open-channel flow. In the absence of periphyton, this flow may be subdivided into three regions (Nezu and Nakagawa 1993): (1) the innermost viscous sublayer, in which the vertical distribution of the longitudinal mean velocity, $\bar{u}(z)$ is linear, i.e., $\bar{u}(z)/u_* = u_*z/\nu$, where u_* is shear velocity, ν is kinematic viscosity, and z is the distance from the bed; (2) the logarithmic layer, in which the longitudinal velocity distribution is semilogarithmic, i.e., $\bar{u}(z)/u_* = (1/\kappa)\ln(z/z_o)$, where κ is the von Karman constant and z_o is the hydrodynamic roughness length; and (3) the outer region, in which mean velocity approaches that of the mainstream above the logarithmic layer and viscous effects are small (Fig. 1). Note that, in Fig. 1, we neglect, for simplicity, the transitional or buffer sublayer between the viscous sublayer and the logarithmic layer. If a solute in the flow is taken up or released by the bed, a DBL will be present within the viscous sublayer. On average, molecular diffusion is faster than turbulent diffusion in the DBL and the solute concentration distribution is approximately linear (Levich 1962; Boudreau 1997, 2001). The thickness of the DBL, $\delta_{Ds} = Sc^{-1/3}\delta_v$, is approximately 1/10th the thickness of the viscous sublayer, $\delta_v = \alpha(\nu/u_*)$, where $\alpha \approx 10$ is a constant, $SC = \nu/D$ is the molecular Schmidt number, and D is the molecular diffusion coefficient for a solute (Levich 1962; Dade 1993; Boudreau 1997). Note that we use δ_{Ds} here

to refer to the thickness of the DBL covering the substratum. We will use δ_{De} below to refer to the thickness of the DBL surrounding a periphyton element.

The appearance of periphyton on the substratum can add a new hydrodynamic layer to the flow organization described above. This layer may lie within the DBL or extend into the overlying part of the viscous sublayer or even above it. We refer to this layer as the canopy layer, following the convention from atmospheric boundary-layer research (e.g., Finnigan 2000). The part of the canopy layer protruding above the viscous sublayer is known as the roughness layer. We postulate that there are three nutrient uptake regimes defined by the interactions between flow hydrodynamics and the periphyton canopy (Fig. 1).

In Regime 1, the periphyton canopy with height h_c is entirely submerged in the substratum DBL, i.e., $\delta_{Ds} \gg h_c$. The biomass-specific uptake rate for this regime, R_{B1} , is defined as

$$R_{B1} = \frac{R_t}{B} = \frac{n_e R_{et}}{n_e b V_e} = \frac{R_e A_e}{b V_e} = \frac{R_e \gamma_1 d_e h_e}{b \gamma_2 d_e^2 h_e} = \frac{\gamma_1}{\gamma_2} \frac{1}{b d_e} \frac{D}{\delta_{De}} \Delta C_{e\infty} = \frac{\gamma_1}{\gamma_2} \frac{1}{b d_e} \frac{D}{\delta_{Ds}} \Delta C_{e\infty} \quad (1)$$

where R_t is the total uptake rate within a fixed bed area; $B = n_e b V_e$ is the total periphyton biomass in the same area; n_e is the number of periphyton elements; b is the periphyton mass density; $V_e = \gamma_2 d_e^2 h_e$ is the element volume; h_e and d_e are the element length and diameter, respectively; $R_{et} = R_e A_e$ is the total uptake rate by an element; $A_e = \gamma_1 d_e h_e$ is the element surface area; γ_1 and γ_2 are shape coefficients representing an element cross-section ($\gamma_1 = \pi$ and $\gamma_2 = \pi/4$ for a circle); $R_e = (D/\delta_{De})\Delta C_{e\infty}$ is the nutrient flux to an element (per unit surface area); δ_{De} is the thickness of the DBL associated with an element; and $\Delta C_{e\infty}$ is the difference between the solute concentration in the fully mixed region above the DBL and the concentration at the element surface. In this regime, δ_{De} may be approximated as δ_{Ds} , i.e., $\delta_{De} \approx \delta_{Ds}$ (Fig. 1). Substituting the standard relationships $\delta_{Ds} = Sc^{-1/3}\delta_v$, $\delta_v = \alpha(\nu/u_*)$, and $u_* = f^{0.5}\bar{u}_r$ (Levich 1962; Dade 1993; Boudreau 1997) in Eq. 1 gives

$$R_{B1} = \frac{\gamma_1}{\gamma_2} \frac{1}{b d_e} \left(\frac{\nu}{D}\right)^{1/3} \frac{u_* D}{\alpha \nu} \Delta C_{e\infty} = \left(\frac{\gamma_1 Sc^{-2/3} u_*}{\gamma_2 \alpha b d_e}\right) \Delta C_{e\infty} = \left(f^{0.5} \frac{\gamma_1 Sc^{-2/3} \bar{u}_c}{\gamma_2 \alpha b d_e}\right) \Delta C_{e\infty} \quad (2)$$

where $f = (u_*/\bar{u}_c)^2$ is the drag coefficient defined for a reference velocity at the top of the periphyton canopy, i.e., $\bar{u}_r = \bar{u}_c$. Equation 2 shows that, for a fixed concentration gradient $\Delta C_{e\infty}$, periphyton diameter, d_e , and drag coefficient, f , uptake rates are linearly proportional to the characteristic flow velocities, u_* and \bar{u}_c , i.e., $R_{B1} \propto u_* \propto \bar{u}_c$.

We describe Regime 3 next, then Regime 2, because the latter represents an intermediate state between Regimes 1 and 3.

In Regime 3, the thickness of the substratum DBL is comparable with the diameters of periphyton elements and much less than the canopy height ($\delta_{Ds} \approx d_e \ll h_c$), so it has little effect on uptake. Instead, uptake is controlled predominately

by the thicknesses δ_{De} of individual DBLs surrounding periphyton elements, which protrude for most of their length above the substratum DBL (Fig. 1). The uptake rate R_{B3} may be parameterized using the same approach used for R_{B1} , and replacing δ_{Ds} with δ_{De} :

$$R_{B3} = \frac{\gamma_1}{\gamma_2} \frac{1}{bd_e} \frac{D}{\delta_{De}} \Delta C_{e\infty} \quad (3)$$

As a first approximation, δ_{De} may be treated as a function of flow velocity, i.e., $\delta_{De} = F_1(\bar{u}_c) = F_2(u_*) = Sc^{-1/3} \delta_v = Sc^{-1/3} \alpha_1 \nu / u_*$, where the coefficient α_1 is similar to α but relates now to the individual elements. Substituting these terms into Eq. 3 gives

$$\begin{aligned} R_{B3} &= \left(\frac{\gamma_1}{\gamma_2} \frac{Sc^{1/3} u_* D}{\alpha_1 b d_e \nu} \right) \Delta C_{e\infty} = \left(\frac{\gamma_1}{\gamma_2} \frac{Sc^{-2/3} u_*}{\alpha_1 b d_e} \right) \Delta C_{e\infty} \\ &= \left(f^{0.5} \frac{\gamma_1}{\gamma_2} \frac{Sc^{-2/3} \bar{u}_c}{\alpha_1 b d_e} \right) \Delta C_{e\infty} \end{aligned} \quad (4)$$

As in Regime 1, Eq. 4 shows that, for a fixed concentration gradient, $\Delta C_{e\infty}$, periphyton diameter, d_e , and resistance coefficient, f , uptake rates are linearly proportional to the characteristic flow velocities, i.e., $R_{B3} \propto u_* \propto \bar{u}_c$. However, the uptake rate R_{B3} is expected to be much higher than R_{B1} :

$$\frac{R_{B3}}{R_{B1}} = \frac{\delta_{Ds1}}{\delta_{De3}} \propto \frac{h_e}{d_e} \gg 1 \quad (5)$$

In Eq. 5, we use the periphyton element length h_e as the scale for the DBL thickness δ_{Ds1} in Regime 1, and the periphyton element diameter d_e as the scale of DBL thickness δ_{De3} for individual elements in Regime 3.

Regime 2 occupies an intermediate position between Regimes 1 and 3 (Fig. 1). In this regime, the thickness of the DBL over the substratum is less than the canopy height but greater than the filament diameter, i.e., $d_e < \delta_{Ds} < h_c$. The uptake rate R_{B2} for this regime is the sum of uptake rates by the portion of the periphyton submerged in the substratum DBL, with length h_{e1} , and the portion protruding above it, with length h_{e2} :

$$\begin{aligned} R_{B2} &= R_{B1} \frac{\delta_{Ds}}{h_c} + R_{B3} \frac{h_c - \delta_{Ds}}{h_c} = \frac{\gamma_1}{\gamma_2} \frac{1}{bd_e} \frac{D}{h_c} \left(1 + \frac{h_c - \delta_{Ds}}{\delta_{De}} \right) \Delta C_{e\infty} \\ &= \frac{\gamma_1}{\gamma_2} \frac{1}{bd_e} \frac{D}{[\delta_{De} h_c / (\delta_{De} + h_c - \delta_{Ds})]} \Delta C_{e\infty} \end{aligned} \quad (6)$$

Note that Eq. 6 uses the approximate relationships $h_{e2}/h_{e1} \approx (h_c - \delta_{Ds})/\delta_{Ds}$ and $h_e/h_{e1} \approx h_c/\delta_{Ds}$. Parameterizations for R_{B1} , R_{B2} , and R_{B3} can now be presented as a single relationship:

$$R_B = \frac{\gamma_1}{\gamma_2} \frac{1}{bd_e} \frac{D}{\delta_{Dg}} \Delta C_{e\infty} \quad (7)$$

where $\delta_{Dg} = \delta_{De} h_c / (\delta_{De} + h_c - \delta_{Ds})$ is the generalized DBL thickness for the periphyton canopy. We use the term generalized thickness because δ_{Dg} can be used to describe each uptake regime: in Regime 1, $\delta_{De} \approx \delta_{Ds}$ and therefore $\delta_{Dg} = \delta_{De} h_c / (\delta_{De} + h_c - \delta_{Ds}) \approx \delta_{Ds}$; in Regime 2, $\delta_{Dg} = \delta_{De} h_c / (\delta_{De} + h_c - \delta_{Ds})$; and in Regime 3, $h_c \gg \delta_{De}$ and $h_c \gg \delta_{Ds}$ and therefore $\delta_{Dg} = \delta_{De} h_c / (\delta_{De} + h_c - \delta_{Ds}) \approx \delta_{De}$. As Eq. 7

indicates, the generalized thickness δ_{Dg} allows us to express the uptake rate R_B using the same relationship for all three regimes.

Uptake rates in Regimes 1 and 3 are predicted to be linearly proportional to the characteristic flow velocities, \bar{u}_c or u_* , as indicated by Eqs. 2 and 4. However, uptake in Regime 2 may vary nonlinearly with velocity, due to nonlinearity in the relationship $h_c = f(u_*$ or $\bar{u}_c)$. Note also that the ratio h_c/δ_{Dg} is proportional to the Peclet number, the ratio of turbulent effects to molecular diffusion effects in mass transport (Levich 1962; Boudreau 1997). Our model suggests that molecular diffusion should control the overall mass transfer of nutrients to the organism surfaces even at very large Peclet numbers.

The preceding model provides a classification of nutrient uptake regimes and a framework within which mass-transfer processes can be assessed. The main uses of the model are to (1) identify the parameters that control nutrient uptake, (2) suggest ways that many of these parameters can be scaled or estimated based on measurable quantities, and (3) predict the form of the relationships between uptake and these parameters. In the following sections, we use the model to assess results of uptake experiments with stream periphyton.

Methods

Periphyton preparation—On each of seven dates between September and December 2002, four acrylic plates (80 × 38 cm, 0.5 cm thick) were attached to a submerged rack in a concrete channel adjacent to the Kaiapoi River, New Zealand. The channel receives river water with an average main-stream velocity of 23 cm s⁻¹. Natural periphyton grew on the plates over 13–26 d, and the plates were rotated every 3–5 d to reduce position effects.

The Kaiapoi River is NO₃ enriched (>500 mg NO₃-N m⁻³), raising the possibility that N-replete periphyton would not take up NO₃ in the flow-tank experiments. To increase periphyton nitrogen demand, the plates were transferred from the channel to large tanks, where they were conditioned for 2 d in 100 liters of aerated, low-nutrient streamwater. Fresh, low-nutrient water was collected from the Kowai River before each experiment. Average nutrient concentrations in the Kowai River water were 15.2 mg NO₃-N m⁻³, 2.5 mg NH₄-N m⁻³, and 1.2 mg DRP m⁻³, giving an average dissolved inorganic N:P ratio of 15:1.

Experimental procedure—Experiments were conducted in a 150-cm-long × 40-cm-wide acrylic flow tank. Water in the tank was circulated from the upper working section to the lower return section with twin propellers connected to a 2.2-kW motor with an Autonics speed controller. Water depth was 8.5 cm, and tank volume was 150 liters. Irradiance was provided by a 1,500 W halogen lamp. Photosynthetically active radiation (PAR) was measured at the periphyton surface with a cosine sensor during each experiment. The average PAR level, 275 μmol m⁻² s⁻¹, is comparable with PAR in unshaded New Zealand streams during the growing season (Young and Huryn 1999).

To begin each experiment, the flow tank was filled with 149 liters of Kowai River water. One of the four periphyton

plates prepared for each date was selected at random, periphyton was scrubbed from the back of the plate, and the plate was screwed back down to the flow-tank test section. The flow was then set to a preselected velocity, and a 1-liter NO_3 + DRP spike was added to the tank. Nutrient spikes were prepared with reagent-grade NaNO_3 and $\text{NaH}_2\text{PO}_4 \cdot 2\text{H}_2\text{O}$ in Kowai River water. Target starting concentrations were 200 $\text{mg NO}_3\text{-N m}^{-3}$, and 15 mg DRP m^{-3} . The target N:P ratio was 14:1, close to that of the water used for conditioning. Water sampling began after waiting 5 min for the nutrient spike to mix completely. Samples were taken with acid-washed syringes, filtered (Whatman GF/F) into acid-washed plastic bottles, and frozen immediately. Experiments were 5 h long, and 10 samples were collected at 15–60-min intervals. Water temperatures during the experiments ranged from 12°C to 16°C. Temperature variation of this magnitude has little effect on diffusivity (Hayduk and Laudie 1974). NO_3 and DRP concentrations in the water samples were measured with a flow-injection analyzer at Hill Laboratories, Hamilton, New Zealand.

After the water samples were collected, periphyton canopy heights were measured in situ. A 40-mm-long needle with a 0.2-mm fluorescent tip was mounted vertically in a micrometer to measure canopy heights with minimal interference by the instrument. The needle was lowered to the canopy surface, 3 cm from the tank wall. The height above the plate at which the needle tip was obscured by periphyton was recorded at 10 points along the plate with 0.2-mm precision. Canopy heights <0.2 mm were assigned values of 0.1 mm.

Following canopy height measurements, the plate was removed from the flow tank and replaced in the conditioning tank. The flow tank was then drained and refilled, and the uptake experiment was repeated with a new plate. The experiment was conducted on two or three plates on each of seven dates. Each of the 16 plates tested was run at a different velocity (range of mean near-bed velocities: 1.1–47.3 cm s^{-1}). Three additional runs were conducted as controls using clean plates at mean near-bed velocities of 1.5, 21.0, and 48.3 cm s^{-1} . The controls were used to assess nutrient flux due to suspended particles. Results of the controls were to be used as correction factors for the periphyton experiments, but no nutrient depletion was detected in the controls, so no corrections were required.

On the morning after each set of experiments, the periphyton plates were reinstalled in the flow tank, and near-bed hydrodynamic characteristics were measured at the same hydraulic conditions used for measuring uptake. These measurements provided flow data that we could relate to uptake rates; they were also used to check for developing boundary layers and secondary currents. The probes of three down-looking Sontek Micro Acoustic Doppler Velocimeters (ADV) were attached to a movable aluminum frame above the tank, in a row parallel to the flow and spaced 10 cm apart. The frame had three screw drives for positioning the probes along the X (longitudinal), Y (transverse), and Z (vertical) axes, with 0.5-mm accuracy on the X and Y axes and 0.1-mm accuracy on the Z axis. Velocities in each axis were measured in a 0.08- cm^3 sampling volume 5 cm below each probe. The sampling volume was maintained at the top of the canopy by adjusting the Z -axis screw drive in 0.1-mm

steps. The ADV sampling frequency was 50 Hz, the duration was 2 min, and the minimum signal-to-noise ratio was 25 dB. If the signal-to-noise ratio fell below 25 dB, Sontek seeding material (hollow glass spheres, 10- μm mean diameter) was added to the tank to enhance ADV performance. A total of 474 velocity time series were logged in binary data files for subsequent processing and analysis.

To reduce ADV measurement time, three levels of measurement effort were employed, comprehensive (40 measurement points at 2-cm intervals on a longitudinal transect down the centerline, plus 54 additional points on nine transverse transects), intermediate (9 points down the centerline, plus 54 points on nine transverse transects), and routine (17 points down the centerline). On each day of ADV measurements, one periphyton plate was comprehensively measured and the rest routinely measured.

In addition to the measurements described above, a single periphyton plate was used to assess the effects of changing near-bed velocities on hydrodynamic parameters and canopy heights while holding periphyton biomass constant. Measurements over this plate were made at seven near-bed velocities ranging from 1.5 to 46.3 cm s^{-1} at the intermediate level of effort.

Following the ADV measurements, periphyton on each plate was sampled to determine biomass levels, which were used to normalize uptake rates and canopy heights (*see Data analysis*) and taxonomic composition. Four periphyton samples were removed from 225- cm^2 areas of each plate with a nylon scraper for biomass (chlorophyll a [$\text{Chl } a$] and periphyton ash-free dry weight) determination. Four additional 225- cm^2 samples were removed and composited for taxonomic analysis. Samples for chlorophyll analysis were prepared by homogenizing in a blender with distilled water, vacuum filtering 10-ml aliquots onto GF/F filters, and extracting pigments in 90% ethanol. $\text{Chl } a$ concentrations were measured with a Jasco 7850 spectrophotometer, using an acidification step (1 mol L^{-1} HCl) to correct for phaeophytin. Ash-free dry weights (AFDWs) were determined by drying samples to constant weight at 60°C and ashing for 4 h at 400°C. The relative abundances of algal taxa were determined using the procedure of Biggs and Smith (2002). Filament diameters and diatom dimensions were measured in each sample with an ocular micrometer.

Data analysis—Uptake rates were calculated as the slopes of linear regressions of nitrate and DRP concentration versus time. In most cases, all 10 nutrient samples were used in each regression. In two runs, single samples were identified as outliers based on deleted residual tests (Kleinbaum et al. 1988) and were omitted.

Near-bed flow parameters were calculated from the ADV data in three steps. First, the data were extracted from the binary files and checked for measurement errors caused by bed interference. Second, measurement errors due to probe misalignments and spikes were detected and corrected. Third, the following parameters were calculated using the corrected data: mean longitudinal (\bar{u}), transverse (\bar{v}), and vertical (\bar{w}) velocities (overbars denote time-averaging); velocity modulus, $\bar{u}_m = (\bar{u}^2 + \bar{v}^2 + \bar{w}^2)^{0.5}$; velocity standard deviations, σ_u , σ_v , and σ_w ; total turbulence energy, $K =$

$0.5(\sigma_u^2 + \sigma_v^2 + \sigma_w^2)$; relative turbulence intensity in the form of σ_u/\bar{u} , σ_v/\bar{u} , σ_w/\bar{u} , and $K^{0.5}/\bar{u}$; and Reynolds stresses, $-u'_i u'_j$, where $\bar{u}'_i = u_i - \bar{u}_i$ and the subscripts i and j stand for longitudinal u , transverse v , and vertical w velocity components. Because the measurements were conducted close to the bed, we used the Reynolds stresses to calculate the local bed shear stresses as $\tau_o/\rho = [\overline{u'w'^2} + \overline{v'w'^2}]^{0.5}$ (Nezu and Nakagawa 1993). Shear velocities were calculated as $u_* = (\tau_o/\rho)^{0.5}$. Detailed procedures for ADV data analysis and interpretation are given in Nikora et al. (2002). Standard errors for each parameter at each position on the periphyton plates were less than 5% of the mean.

The thicknesses of substratum DBLs were calculated as $\delta_{Ds} = Sc^{-1/3}\delta_v$ (see *Conceptual framework*). We then used the ratio h_c/δ_D to identify the uptake regime in effect during each experiment (Fig. 1). From the measured values of u_* and h_c , and neglecting errors in α , ν , and D , we calculated errors in our estimates of h_c/δ_D ; errors ranged from 6% to 30% and averaged 20% (Schenk 1972).

Results

Flow conditions—Near-bed flow conditions can be described most concisely using data for the single plate exposed to seven near-bed velocities. This eliminates the confounding effect of varied periphyton biomass among plates. Longitudinal distributions of mean near-bed velocity, total turbulence energy, bed shear stress, and relative turbulence intensity (as $K^{0.5}/\bar{u}$) are shown in Fig. 2. For clarity, the data for two of the seven flow rates measured are shown in Fig. 2, with mean near-bed velocities of 46.3 cm s⁻¹ (the fastest), and 7.5 cm s⁻¹ (the second slowest). At each longitudinal position, seven points are shown for each velocity, corresponding to the seven measurements made on each transverse transect. There were no systematic changes in flow parameters along the longitudinal or transverse axes and no indications of developing boundary layers or secondary currents.

Spatial variability of the hydrodynamic parameters across the experimental plates was generally low; with few exceptions, coefficients of variation for each parameter were less than 0.5 (Table 1). Relatively low spatial variation justifies the use of spatially averaged values for the hydrodynamic parameters in the following analysis of nutrient uptake. Cross-correlations between hydrodynamic parameters indicated that shear velocity was highly correlated with near-bed turbulence properties, as expected (Nezu and Nakagawa 1993). Therefore, we used two spatially averaged parameters in our analyses, near-bed mean velocity and shear velocity. The roughness Reynolds number, $Re_* = (u_* h_c/\nu)$, ranged from 5 to 60, indicating that flow conditions in our experiments were transitional at low velocities and hydraulically rough at high velocities (Nezu and Nakagawa 1993).

Periphyton assemblages—The dominant periphyton taxa on the acrylic plates are listed in Table 1. These taxa accounted for at least 75% of the periphyton cover. The most common morphological forms were filaments (*Ulothrix zonata*, *Draparnaldia* sp.), erect clusters of axially attached diatoms (*Synedra* spp.), mat-forming diatoms (*Cymbella kap-*

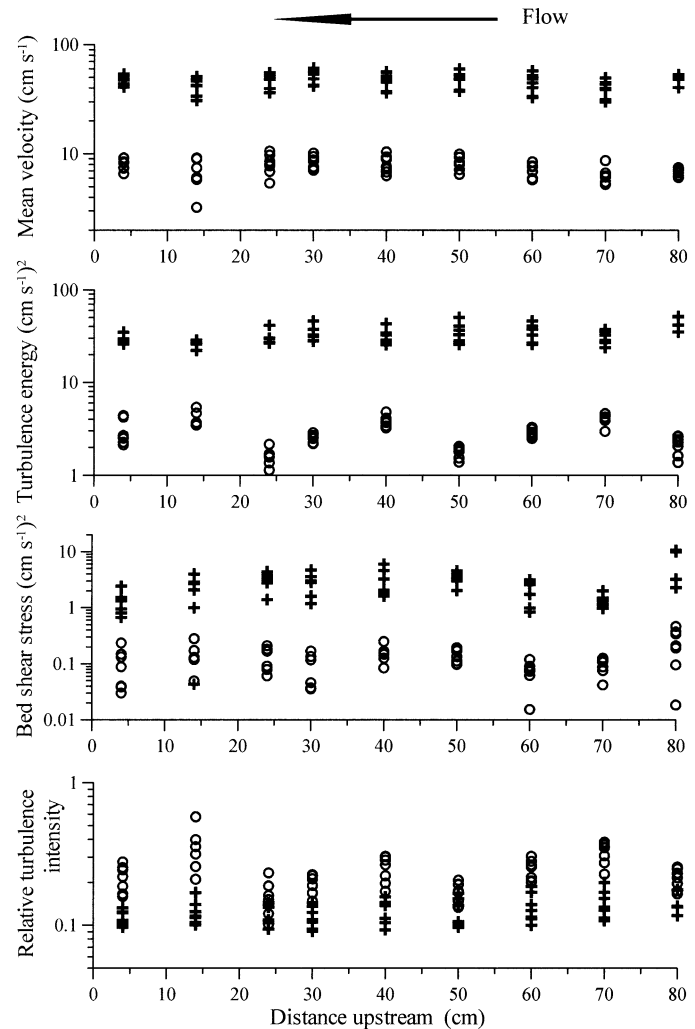


Fig. 2. Longitudinal distributions of mean near-bed velocities, \bar{u} ; total turbulence energy, $k = 0.5(\sigma_u^2 + \sigma_v^2 + \sigma_w^2)$; bed shear stress, $\tau_o/\rho = (\overline{u'w'^2} + \overline{v'w'^2})^{0.5}$; and relative turbulence intensity, $K^{0.5}/\bar{u}$ along a periphyton-covered plate. Data are for two near-bed velocities: 46.3 cm s⁻¹ (crosses) and 7.5 cm s⁻¹ (circles). At each longitudinal position, values for seven ADV measurements at evenly spaced transverse positions are shown.

pii, *Acanthidium* spp.), stalked and filament-forming diatoms (*Gomphonema truncatum*, *Encyonema minutum*), and hemispherical colonies (*Gloeocystis* sp.). Mean in situ canopy heights ranged from <0.2 to 4 mm (Table 1). As there were no systematic changes in canopy height along the longitudinal axes of the plates, we used mean canopy heights in subsequent data analyses. Canopy heights decreased with increases in near-bed velocity and shear velocity (Fig. 3). The negative slopes in Fig. 3 indicate increased canopy bending with increasing velocity. Nikora et al. (1998) predicted that periphyton bending increases as a power function of the shear velocity, and our data support this prediction.

Nutrient uptake and identification of uptake regime—Biomass-specific uptake rates in the experiments ranged from 0.01 to 0.07 mg NO₃-N mg Chl a⁻¹ min⁻¹ and 0.004–0.019

Table 1. Flow and periphyton parameter values in the uptake experiments. Values are means (1 SD). Dominant (>5% relative abundance) periphytic algal taxa are ordered from most to least abundant from left to right. In situ canopy heights on last five plates were all <0.2 mm.

Experiment	Near-bed velocity (cm s ⁻¹)	Shear velocity (cm s ⁻¹)	Relative turbulence intensity	Turbulence energy (cm ² s ⁻²)	Canopy height (mm)	Chlorophyll <i>a</i> (mg m ⁻²)	AFDW (mg m ⁻²)	Most abundant taxa*
1	28.8 (1.9)	2.3 (0.3)	0.2 (0.02)	29.2 (4.0)	1.5 (1.4)	3.2 (0.8)	891 (89)	Uz Sa Sr
2	4.4 (0.4)	0.3 (0.1)	0.3 (0.09)	2.0 (1.3)	2.5 (0.5)	3.3 (0.7)	1009 (293)	Uz Sa G
3	15.3 (4.0)	1.3 (0.3)	0.2 (0.09)	11.6 (3.1)	4.0 (1.7)	6.2 (0.6)	1721 (310)	Uz Sa G
4	8.0 (1.2)	0.5 (0.2)	0.2 (0.07)	3.5 (1.8)	1.0 (0.2)	3.8 (0.2)	814 (44)	Uz Sa Al
5	24.5 (0.9)	1.7 (0.2)	0.2 (0.01)	18.0 (2.1)	0.5 (0.3)	2.1 (0.4)	694 (182)	Uz Sa G
6	35.4 (1.4)	2.6 (0.4)	0.2 (0.01)	34.7 (5.5)	0.9 (0.6)	4.0 (2.0)	1152 (346)	Uz Sa Al
7	14.8 (1.9)	1.1 (0.3)	0.2 (0.03)	12.0 (2.5)	1.0 (0.9)	4.1 (1.4)	1695 (512)	Uz Sa G
8	5.7 (1.6)	0.6 (0.2)	0.4 (0.1)	4.3 (0.8)	1.9 (0.7)	4.5 (1.6)	1646 (746)	Uz Sa Na
9	38.1 (7.8)	2.2 (0.7)	0.2 (0.04)	34.4 (10.9)	1.1 (0.9)	3.4 (0.6)	1076 (345)	Uz Sa G
10	17.0 (4.0)	1.0 (0.4)	0.2 (0.05)	11.0 (2.5)	1.1 (0.7)	4.4 (0.8)	939 (57)	Uz Sa Ck
11	1.1 (0.4)	0.4 (0.2)	1.4 (0.7)	2.1 (1.4)	2.0 (1.7)	3.1 (1.1)	518 (140)	Uz Sa Ck
12	9.8 (1.7)	0.5 (0.2)	0.2 (0.06)	4.3 (2.5)	0.1	1.0 (0.6)	297 (121)	Uz Sa Sr
13	21.1 (2.7)	1.0 (0.4)	0.2 (0.02)	12.9 (3.1)	0.1	0.9 (0.3)	321 (114)	Uz Sa Em
14	47.3 (11.7)	2.1 (1.6)	0.2 (0.1)	68.4 (68.4)	0.1	1.8 (0.6)	829 (310)	Uz Sa D
15	38.1 (7.5)	1.9 (0.9)	0.2 (0.04)	45.3 (21.6)	0.1	3.7 (1.8)	1480 (377)	Uz Sa Em
16	26.5 (3.4)	1.4 (0.6)	0.2 (0.02)	23.7 (7.3)	0.1	3.2 (1.5)	1411 (536)	Uz Sa G

* Periphyton taxa. Chlorophyta: Uz, *Ulothrix zonata*; D, *Draparnaldia* sp.; G, *Gloeocystis* sp. Bacillariophyta: Sa, *Synedra acus*; Sr, *Synedra rumpens*; Ck, *Cymbella kappii*; Al, *Acanthidium linearis*; Na, *Nitzschia acicularis*; Em, *Encyonema minutum*; Am, *Acanthidium minutissimum*.

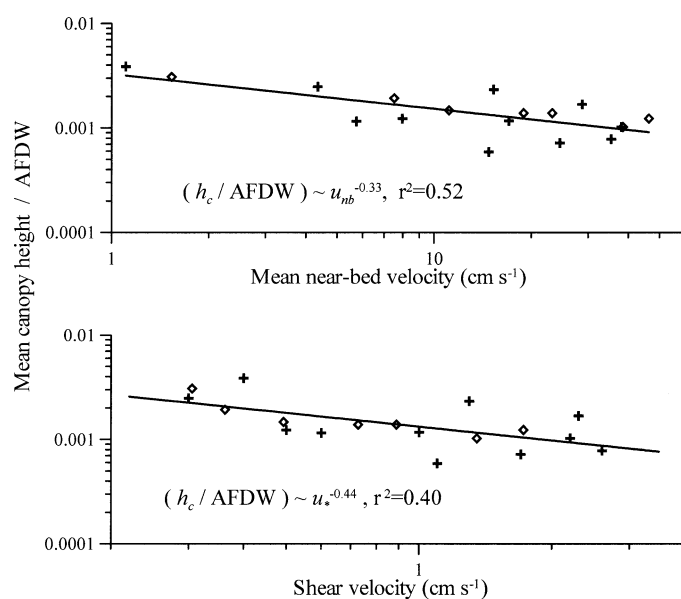


Fig. 3. Periphyton canopy height versus near-bed velocity and shear velocity. Canopy heights are normalized by periphyton AFDW to remove the effects of among-plate differences in biomass. Points are from individual uptake experiments (crosses) and the single plate exposed to seven velocities (diamonds). Data for canopy heights <0.2 mm are not shown. Lines are for exponential regression equations. For near-bed velocity, $p = 0.001$; for shear velocity, $p = 0.005$.

mg DRP mg Chl *a*⁻¹ min^{-1b}. Uptake rates of both nutrients increased linearly with both near-bed velocity and shear velocity (Fig. 4), which is consistent with the conceptual model. These results indicate that uptake was mass-transfer limited over the velocity range used (near-bed velocity range: 1.1–47.3 cm s⁻¹, u_* range: 0.4–2.6 cm s⁻¹). There was no indication that a saturating velocity was approached at which uptake would shift to kinetic control. Uptake was not concentration dependent, as indicated by linear decreases in NO₃ and DRP concentrations in each experiment over time. All linear regressions of NO₃ and DRP concentration on time were significant ($p < 0.03$) and had r^2 values >0.6. The lack of concentration dependence was likely due to large ratios of water volume to periphyton biomass (range: 70–732 L mg⁻¹ periphyton Chl *a*). NO₃ depletion during the experiments ranged from 4% to 18%, and DRP depletion ranged from 13% to 54%. No detectable NO₃ or DRP flux occurred during the control runs.

Two lines of evidence indicate that NO₃ and DRP uptake in the flow-tank experiments occurred in mass-transfer Regime 3 (Fig. 1). First, a large proportion of the periphyton canopy protruded from the substratum DBL in each experiment, as indicated by h_c/δ_{D_s} values of 4–60 (Fig. 5). Canopies were not submerged in the substratum DBL, as we expect for Regime 1. Second, uptake rates did not vary systematically with canopy height relative to substratum DBL thickness (h_c/δ_{D_s}), as we expect for Regime 2 (Fig. 5).

Discussion

The idea that increased velocity reduces viscous layer thickness and enhances nutrient uptake by algae was pro-

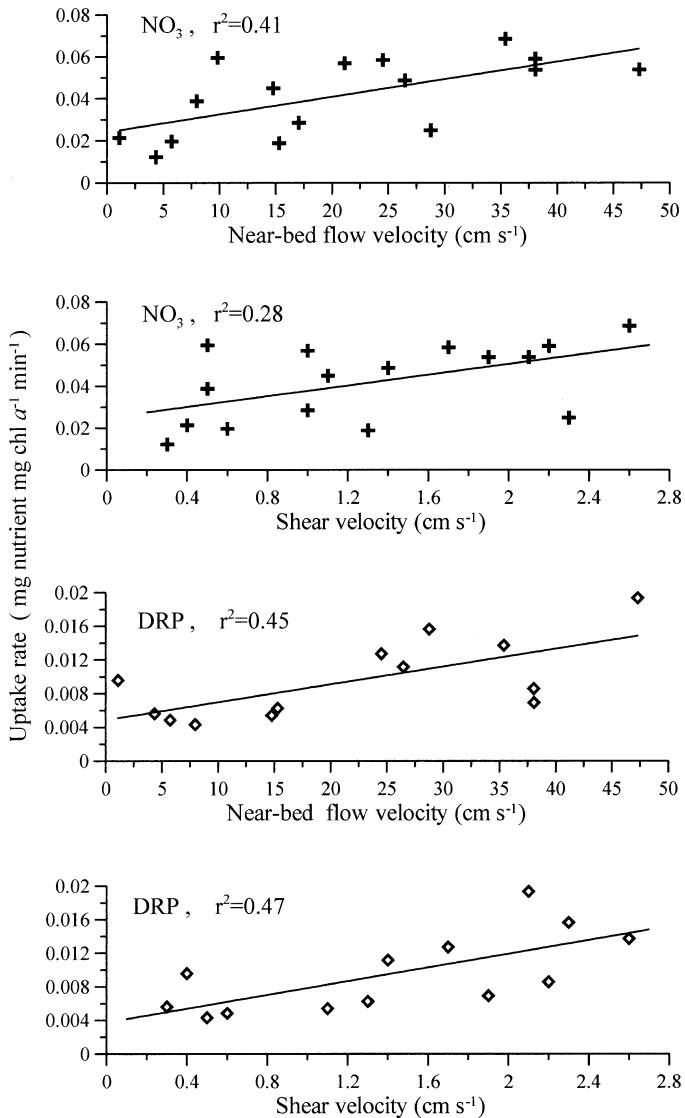


Fig. 4. Biomass-specific nitrate and DRP uptake rates versus spatially-averaged near-bed velocity and shear velocity. Lines are for linear regression equations. All regression slopes were significantly different than zero ($p < 0.05$).

posed over 50 yr ago (Munk and Riley 1952). Positive relationships between nutrient uptake by lotic algae and water velocity have been reported for 40 yr (e.g., Whitford and Schumacher 1961). However, theoretical descriptions of the variables that control nutrient mass transfer to lotic algae have been lacking. The model presented here is intended to provide one such description for the case of fully developed boundary layers and flat substrata.

Regime 3 of our mass-transfer model provides a good description of the flow-tank experiment results: NO_3 and DRP uptake rates increased linearly with near-bed and shear velocity, uptake was independent of h_c/δ_{Ds} , and h_c/δ_{Ds} ratios were ≥ 4 , suggesting that 75% or more of the canopy protruded from the substratum DBL. The results were not entirely the ones we anticipated, however; we used a wide range of near-bed velocities, with the expectation that two

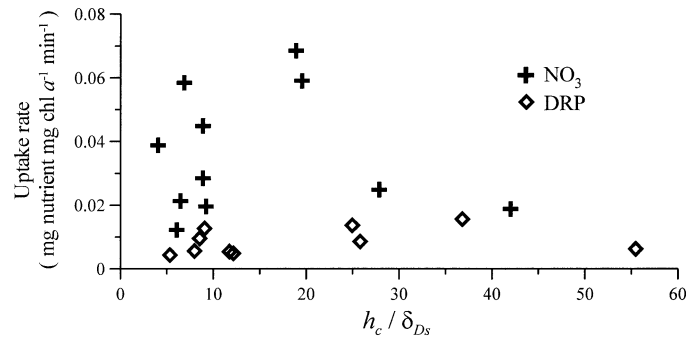


Fig. 5. Biomass-specific nitrate and DRP uptake rates versus periphyton canopy height relative to substratum DBL thickness. The ratio h_c/δ_{Ds} indicates the degree to which the canopy extends from the DBL into the upper flow region. Data for canopy heights < 0.2 mm are not shown.

or three of the regimes shown in Fig. 1 would be represented. Further, we anticipated that uptake would shift from mass-transfer control to kinetic control at the highest velocities. This was not the case. The hydraulic conditions under which Regime 3 is in effect for short periphyton assemblages appear to span a near-bed velocity range of at least an order of magnitude. Comparisons with studies that used near-bed velocities out of the range that we used could help characterize the limits of the uptake regimes. However, few studies include sufficient information (e.g., canopy heights, DBL dimensions) or used comparable open-channel flow conditions. In a study of carbon dioxide uptake by epiphytic periphyton in closed containers, Jones et al. (2000) reported DBL thicknesses of 0.8–2.4 mm and periphyton thicknesses of 0.1–1.1 mm. Periphyton thickness was measured using the same technique we used for canopy heights, so we can compare h_c/δ_{Ds} ratios. For the epiphytic periphyton, h_c/δ_{Ds} ranged from 0.1 to 0.4, an order of magnitude below our lowest values. Near-substratum flow conditions were not reported by Jones et al. (2000), but their low h_c/δ_{Ds} values suggest that carbon dioxide uptake was in our Regime 1 or 2.

A study of mass-transfer-limited oxygen uptake by a salt-pond periphyton mat over a range of flow velocities (Jørgensen and Des Marais 1990) is more comparable with ours. Uptake rates by the salt-pond mat increased with velocity from 0.3 to 7.7 cm s^{-1} , while δ_{Ds} decreased from 0.6 to 0.2 mm. If the topographic high points of the mat (0.9–1.1 mm) are considered equivalent to canopy heights, the h_c/δ_{Ds} ratio ranged from about 1.5 at low velocities to 6 at high velocities. These results suggest that oxygen uptake was in our Regime 2 at the lowest velocities used and in our Regime 3 at the highest velocities.

Our results, and those of Jørgensen and Des Marais (1990), lead to two general propositions. First, near-bed flow over periphyton must be extremely slow for substratum DBLs to develop that cover the canopy deeply ($\delta_{Ds} \gg h_c$), and control mass transfer (Fig. 1, Regime 1). This appears to be a rare situation for thin periphyton assemblages and will be even rarer for thick algal mats or erect bryophytes and macrophytes in streams. In the latter cases, the topography of the DBL closely follows that of organism surfaces, even at low velocities (Jørgensen 2001, Røy et al. 2002).

The occurrence of Regime 1 in lotic systems may be limited to backwaters and alcoves where water velocities and turbulent mixing can be very slow, as indicated by tracer experiments (Carling 1992; Fernald et al. 2001).

Second, saturating velocities may be very high for periphyton assemblages in natural streams. Saturating velocities reported for dissolved inorganic nitrogen and DRP uptake by macroalgae are $<20 \text{ cm s}^{-1}$ (Gerard 1982; Borchardt et al. 1994; Hurd et al. 1996). We predict that saturating velocities for periphyton will be much higher, based on our observations of mass-transfer limitation at mainstream velocities $>50 \text{ cm s}^{-1}$ and on reports of increased periphyton biomass accrual (and consequently, nutrient uptake) with increasing velocity up to 150 cm s^{-1} (Horner et al. 1990; Biggs and Hickey 1994). Drag forces sufficient to remove periphyton from substrata may occur at much lower velocities (Biggs and Thomsen 1995). If nutrient uptake to periphyton in natural streams increases with velocity to the point where periphyton is dislodged, then mass transfer is always the rate-limiting step for uptake. For periphyton that are highly resistant to dislodgement, the rate-limiting step for uptake may shift from mass transfer to membrane transport at high velocities (Sanford and Crawford 2000).

Other than bending and consequent changes in canopy height, we have not addressed morphological responses of periphyton to changing velocities or the effects of those responses on nutrient uptake. Several responses could affect uptake, including reconfiguration (streamlining) and fluttering by flexible elements. Streamlining in response to increased drag may increase packing of elements (Sheath and Hambrook 1988). Koehl and Alberte (1988) observed reductions in carbon uptake by a marine macroalga as a result of streamlining. This effect may be due to coalescence of the DBLs surrounding each element and/or reduced penetration of turbulent eddies into the canopy. Conversely, fluttering may enhance uptake by reducing δ_D (Stevens et al. 2003). Enhanced nutrient uptake has been reported for fluttering marine macroalgae (Koehl and Alberte 1988; Denny and Roberson 2002) but not for periphyton. These effects are not accounted for in our model and could cause deviations from the proposed linear relationships between uptake and flow parameters.

Based on the conceptual model presented here, we predict that nutrient transport to periphyton taxa with elongate morphologies (e.g., filaments and stalked diatoms) will be higher than to prostrate taxa (e.g., crusts and prostrate diatoms), as elongate taxa extend relatively more absorptive tissue into turbulent flow. In oligotrophic water where growth is nutrient-limited, elongate growth may be viewed as a strategy for maximizing nutrient acquisition (Biggs et al. 1998b). Stream periphyton that epitomize this strategy have uniseriate filaments (e.g., *Ulothrix* and *Draparnaldia*), which maximize both length and surface:volume ratio per unit biomass. However, elongate forms also experience higher drag forces than prostrate forms and risk greater losses by dislodging or breakage (Biggs and Thomsen 1995).

The trade-off between enhanced mass transfer and resistance to drag is summarized in the following hypothesis: long filamentous periphyton dominate low-velocity areas, where viscous effects are great but drag forces are low; pros-

trate periphyton dominate high-velocity regions, where viscous effects are reduced but drag forces are greater; and periphyton of intermediate stature, such as stalked and filamentous diatom mats, dominate areas with intermediate velocities, where the benefits of nutrient mass transfer and the costs of drag forces are more nearly balanced. A survey of periphyton growth forms by Biggs et al. (1998a) provides circumstantial evidence for the hypothesis: as velocity increased, prostrate periphyton biomass increased monotonically and long filamentous periphyton decreased monotonically. Stalked and filamentous diatoms had peak biomass levels at intermediate velocities. There is no clear threshold separating low and high mainstream velocities in the preceding hypothesis. Optimal velocities for growth will vary with nutrient concentrations and periphyton stature. High nutrient concentrations reduce the benefits associated with increased velocities because nutrient loading may reduce physiological demand (Borchardt et al. 1994) and because increased concentrations cause increased diffusion rates. If periphyton stature changes over time due to growth or removal, changes in h_c/δ_{D_s} and in h_c/δ_v will cause optimal velocities to change as well.

Although the model presented here concerns uptake by periphyton in fully developed flows over flat substrata, it can be modified to encompass developing boundary layers and rough substrata. In the case of developing boundary layers, the characteristic velocity and the thickness of each hydrodynamic layer change with distance from a leading edge (Levich 1962), so longitudinal position must be specified for some parameters (e.g., δ_{D_e} and δ_{D_s}). The case of rough substrata will require additional terms in the model that express the ratio of the periphyton canopy height to the substratum roughness height (Nikora et al. 2002).

References

- BIGGS, B. J. F., D. G. GORING, AND V. I. NIKORA. 1998a. Subsidy and stress responses of stream periphyton to gradients in water velocity as a function of community growth form. *J. Phycol.* **34**: 598–607.
- , AND C. W. HICKEY. 1994. Periphyton responses to a hydraulic gradient in a regulated New Zealand river. *Freshw. Biol.* **24**: 49–59.
- , AND R. A. SMITH. 2002. Taxonomic richness of stream benthic algae: Effects of flood disturbance and nutrients. *Limnol. Oceanogr.* **47**: 1175–1186.
- , R. J. STEVENSON, AND R. L. LOWE. 1998b. A habitat matrix conceptual model for stream periphyton. *Arch. Hydrobiol.* **143**: 21–56.
- , AND H. A. THOMSEN. 1995. Disturbance of stream periphyton by perturbations in shear stress: Time to structural failure and differences in community resistance. *J. Phycol.* **31**: 233–241.
- BORCHARDT, M. A., J. P. HOFFMANN, AND P. W. COOK. 1994. Phosphorus uptake kinetics of *Spirogyra fluviatilis* (Charophyceae) in flowing water. *J. Phycol.* **30**: 403–417.
- BOUDREAU, B. P. 1997. Diagenetic models and their implementation. Modeling transport and reactions in aquatic sediments. Springer.
- . 2001. Solute transport above the sediment–water interface, p. 104–126. *In* B. P. Boudreau and B. B. Jørgensen [eds.], *The benthic boundary layer*. Oxford Univ. Press.

- CARLING, P. A. 1992. In-stream hydraulics and sediment transport, p. 101–125. In P. Calow and G. E. Petts [eds.], *The rivers handbook*, v. 1. Blackwell Scientific.
- DADE, W. B. 1993. Near-bed turbulence and hydrodynamic control of diffusional mass transfer at the sea floor. *Limnol. Oceanogr.* **38**: 52–69.
- DENNY, M. W., AND L. ROBERSON. 2002. Blade motion and nutrient flux to the kelp *Eisenia arborea*. *Biol. Bull.* **203**: 1–13.
- FERNALD, A. G., P. J. WIGINGTON, AND D. H. LANDERS. 2001. Transient storage and hyporheic flow along the Willamette River, Oregon: Field measurements and model estimates. *Water Res.* **37**: 1681–1694.
- FINNIGAN, J. 2000. Turbulence in plant canopies. *Ann. Rev. Fluid Mech.* **32**: 519–571.
- GERARD, V. 1982. In situ water motion and nutrient uptake by the giant kelp *Macrocystis pyrifera*. *Mar. Biol.* **69**: 51–54.
- HAYDUK, W., AND H. LAUDIE. 1974. Prediction of diffusion coefficients for nonelectrolytes in dilute aqueous solutions. *Am. Inst. Chem. Eng. J.* **20**: 611–615.
- HORNER, R. R., E. B. WELCH, M. R. SEELEY, AND J. M. JACOBY. 1990. Responses of periphyton to changes in current velocity, suspended sediment and phosphorus concentration. *Freshw. Biol.* **24**: 215–232.
- HURD, C. L., P. J. HARRISON, AND L. D. DRUEHL. 1996. Effect of seawater velocity on inorganic nitrogen uptake by morphologically distinct forms of *Macrocystis integrifolia* from wave-sheltered and exposed sites. *Mar. Biol.* **126**: 205–214.
- JONES, J. I., J. W. EATON, AND K. HARDWICK. 2000. The influence of periphyton on boundary layer conditions: A pH microelectrode investigation. *Aq. Bot.* **67**: 191–206.
- JØRGENSEN, B. B. 2001. Life in the diffusive boundary layer, p. 348–373. In B. P. Boudreau and B. B. Jørgensen [eds.], *The benthic boundary layer*. Oxford Univ. Press.
- , AND D. DES MARAIS. 1990. The diffusive boundary layer of sediments: Oxygen microgradients over a microbial mat. *Limnol. Oceanogr.* **35**: 1343–1355.
- JUMARS, P. A., J. E. ECKMAN, AND E. KOCH. 2001. Macroscopic animals and plants in benthic flows, p. 320–347. In B. P. Boudreau and B. B. Jørgensen [eds.], *The benthic boundary layer*. Oxford Univ. Press.
- KLEINBAUM, D. G., L. L. KUPPER, AND K. E. MULLER. 1988. Applied regression analysis and other multivariable methods, 2nd ed. PWS-Kent.
- KOCH, E. W. 1993. The effect of water flow on photosynthetic processes of the alga *Ulva lactuca* L. *Hydrobiologia* **260/261**: 457–462.
- KOEHL, M. A. R., AND R. S. ALBERTE. 1988. Flow, flapping and photosynthesis of *Nereocystis luetkeana*: A functional comparison of undulate and flat blade morphologies. *Mar. Biol.* **99**: 435–444.
- LEVICH, V. G. 1962. *Physicochemical hydrodynamics*. Prentice-Hall.
- MUNK, W., AND G. A. RILEY. 1952. Absorption of nutrients by aquatic plants. *J. Mar. Res.* **11**: 215–240.
- NEZU, I., AND H. NAKAGAWA. 1993. Turbulence in open-channel flows. A. A. Balkema.
- NIKORA, V. I., D. G. GORING, AND B. J. F. BIGGS. 1998. A simple model of stream periphyton-flow interactions. *Oikos* **81**: 607–611.
- , ———, AND ———. 2002. Some observations of the effects of micro-organisms growing on the bed of an open channel on the turbulence properties. *J. Fluid Mech.* **450**: 317–341.
- NOBEL, P. S. 1999. *Physicochemical and environmental plant physiology*, 2nd ed. Academic.
- RIBER, H. H., AND R. G. WETZEL. 1987. Boundary-layer and internal diffusion effects on phosphorus fluxes in lake periphyton. *Limnol. Oceanogr.* **32**: 1181–1194.
- RØY, H., M. HÜTTEL, AND B. B. JØRGENSEN. 2002. The role of small-scale sediment topography for oxygen flux across the diffusive boundary layer. *Limnol. Oceanogr.* **47**: 837–847.
- SANFORD, L. P., AND S. M. CRAWFORD. 2000. Mass transfer versus kinetic control of uptake across solid-water boundaries. *Limnol. Oceanogr.* **45**: 1180–1186.
- SCHENCK, H. 1972. *Theories of engineering experimentation*. McGraw Hill.
- SHEATH, R. G., AND J. A. HAMBROOK. 1988. Mechanical adaptations to flow in freshwater red algae. *J. Phycol.* **24**: 107–111.
- STEVENS, C. L., C. L. HURD, AND P. E. ISACHSEN. 2003. Modelling of diffusion boundary layers in subtidal macroalgal canopies: The response to waves and currents. *Aquat. Sci.* **65**: 81–91.
- WHEELER, W. N. 1980. Effect of boundary layer transport on the fixation of carbon by the giant kelp *Macrocystis pyrifera*. *Mar. Biol.* **56**: 103–110.
- WHITFORD, L. A., AND G. J. SCHUMACHER. 1961. Effect of current on mineral uptake and respiration by a freshwater alga. *Limnol. Oceanogr.* **6**: 423–425.
- YOUNG, R. A., AND A. D. HURYN. 1999. Effects of land use on stream metabolism and organic matter turnover. *Ecol. Appl.* **9**: 1359–1376.

Received: 20 December 2003

Accepted: 2 June 2004

Amended: 28 June 2004